

Viscous fingering: A singularity in Laplacian growth models

Martine Ben Amar

Laboratoire de Physique Statistique, Ecole Normale Supérieure, 24 rue Lhomond, 75231 Paris Cedex 05, France

(Received 3 October 1994)

The η model in the linear or radial geometry is investigated numerically. It turns out that the main characteristics of the viscous fingering instability ($\eta=1$) at vanishing capillary number such as the $\lambda=\frac{1}{2}$ limit are not recovered. For $\eta\neq 1$, the selected finger width decreases with the capillary parameter, indicating the formation of needlelike structures.

PACS number(s): 47.20.Hw, 68.10.-m

The Saffman-Taylor (ST) viscous fingering instability [1] can be seen as an archetype of a pattern forming system. In a typical experiment, one pushes a viscous fluid by a less viscous one, between two parallel plates, either in the linear or in the circular geometry. It has been the subject of a very large number of studies [1] during the last decade which led to two major results, characteristic of the low capillary or high growth-rate domain. The first result concerns the linear geometry and the so-called $\lambda=\frac{1}{2}$ limit [1-3]: at constant flux, one observes a steady finger with a width relative to the cell width $2a$ called λ and a constant velocity U . As one decreases the capillary number given by $\sigma=b^2T/12\Delta Ua^2$ (with b the distance between the plates, Δ the viscosity contrast, and T the surface tension) by increasing the finger velocity, one observes that the width λ decreases from 1 to $\frac{1}{2}$. The second important result concerns the dynamics of the radial growth. Experimentally, at short times t , one observes a self-similar regime in $t^{1/2}$ [4] followed by a breakdown of this regime at a finite time due to a tip-splitting instability. This process, when repeated, is responsible for the fractal pattern observed at very long times. A spatial anisotropy of the surface tension (artificially introduced in a viscous flow experiment in order to mimic a crystal-growth process) destroys these two results [5], leading to stable sharp-pointed structures in both geometries: linear or circular. It is observed that, in the presence of anisotropy, the characteristic length scale of the pattern, when compared to the size of the cell, goes to zero with the capillary parameter σ .

The viscous fingering problem can be included in a more general class of Laplacian growth model: the η model. One keeps the usual Gibbs-Thomson condition $\Phi_{\text{int}}=-\sigma\kappa$ on the interface (Φ is the dimensionless Laplacian field while κ is the dimensionless curvature). However, it generalizes the Stefan condition, which usually relates the finger velocity U to the Laplacian fluid Φ . In dimensionless units, one gets

$$\mathbf{e}_x \cdot \mathbf{n} = (\mathbf{n} \cdot \nabla \Phi)^\eta \quad (1)$$

with \mathbf{n} the normal unit vector and \mathbf{e}_x the unit vector along the cell axis. Of course, this modified Stefan relation is no longer a continuity equation for the velocity field as it is in viscous fingering (which corresponds to $\eta=1$). However, such a boundary condition appears to apply to dielectric breakdown [6], non-Newtonian viscous fingering such as in clays or polymer solutions in the power law regime [6] and is also very often used in numerical simulations of diffusion limited

aggregation (DLA) [7]. Moreover, the η model is the most obvious and the simplest deviation from the usual model so that one would expect only small deviations concerning the physical results, especially if η is close to 1. By numerical means, we show here that the $\eta=1$ model is completely singular and that for small σ , small-scale structures like needles are formed, for $\eta<1$ and $\eta>1$. In some sense, one recovers results similar to those for a fourfold anisotropic surface tension although the analogy immediately stops here. A decrease of λ below $\frac{1}{2}$ has also been observed when one incorporates a thin film effect [8].

A classical first step in any analytical or numerical treatment consists in trying to find the zero-surface-tension set of solutions for the profile shape. For the particular value $\eta=1$, one knows exact solutions in the linear [1] and in the confined radial geometry [9] (wedge-shaped cell). In both geometries, the relative width of the fingers cannot be predicted in the absence of a surface tension T . Once introduced, even infinitesimally small, surface tension selects a value for λ that is close to $\frac{1}{2}$ for high speeds [2,3]. In radial growth the situation is even more complicated since, with capillarity, a solution exists only above a capillary number threshold [9]. Near this threshold, the λ value is close to $\frac{1}{2}$ if the sector angle θ_0 of the wedge is weak but λ is an increasing function of the sector angle θ_0 and is typically of the order of 0.85 for $\theta_0=90^\circ$.

We present first our numerics which are the main results of this paper. We adapt the hodograph method of McLean and Saffman (MS) [2] which maps the flow domain onto an upper half-space Σ defined by $\Sigma=s+it$. In this plane, the walls of the cell occupy the real negative axis, the steady interface is represented by the segment $[0,1]$ and the cell axis by $[1,\infty]$. Since this method and its extension to the radial geometry have been discussed in detail before [9], we only recall the main equations for the modified complex velocity $qe^{-i\tau}$ for the linear geometry and refer to [9] for the radial geometry. For the linear channel, the equation then reads

$$\kappa qs \frac{d}{ds} qs \frac{d\tau}{ds} - q = \frac{q}{(1-\lambda)} + \frac{q}{\pi Q_0/\lambda} \int_0^1 ds' \frac{(-\sin\tau)^\mu}{q(s'-s)}, \quad (2)$$

with $\kappa=4\pi^2\sigma\lambda/Q_0(1-\lambda)^2$; Q_0 is the dimensionless flux, τ is the angle between the cell axis and the tangent to the interface. The boundary conditions for the complex velocity $qe^{-i\tau}$ are $\tau(0)=0$, $\tau(1)=-\pi/2$, $q(0)=1$, and $q(1)=0$.

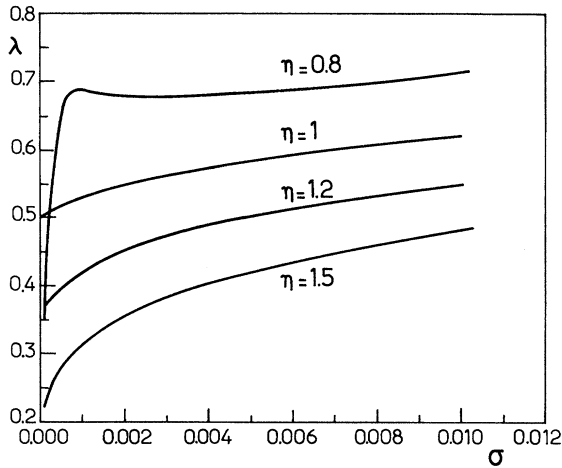


FIG. 1. The selected width λ for different η as a function of σ in the channel geometry. The viscous fingering $\eta=1$ is indicated for reference.

For $\mu = 1/\eta = 1$, one recovers the MS equations, since the right-hand side of Eq. (1) is simply $-\cos\tau$ in this case. For the wedge geometry, one needs to modify the equivalent equation established in [9] by introducing the power μ for the sine term as in Eq. (2). Since both q and τ are unknown, a new relation is necessary which is provided by analyticity properties [2,9].

For vanishing σ , and for $\eta > 0.5$, one obtains a continuous set of solutions with all possible relative finger widths: $0 < \lambda < 1$. The set of solutions disappears for $\eta < 0.5$. The case $\eta = 0.5$ appears to be a marginal one since numerical solutions can only be obtained for $\lambda > 0.5$. As η is decreasing, the finger tip appears more and more sharp-pointed and for $\eta = 0.5$, the tip nearly shows a cusp, which would correspond to an unphysical situation. With increasing η , the zero-surface-tension profiles show a rather flat tip. All η values greater than 0.5 seem equivalent since a continuous set of solutions with arbitrary relative width, $0 < \lambda < 1$, can be found numerically. We do not present here the profiles which are modified by surface tension, especially when $\lambda > 0.5$.

With surface tension, the solutions which are well behaved at the tip and at infinity form a discrete set at a fixed σ : the relative width λ is selected. Here, we focus only on the first eigenvalue λ which corresponds to the experimentally observable situation. In Fig. 1, we show the calculated eigenvalue spectrum for different η values around 1. For η greater than 1, λ increases smoothly with σ . At a small but finite σ , λ is close to 0.5 but always remains smaller than the ST corresponding value. From Fig. 1, one can notice the existence of two different regimes. The first regime occurs when both λ and σ are close to 0. This regime does not exist for the ST case since $\lambda = \frac{1}{2}$ for $\sigma = 0^+$. In the second regime, at greater capillary parameter, the λ spectrum is similar to the ST one [2]. These two regimes are separated by a crossover regime which appears more clearly for η close to 1. For $\eta < 1$ and σ finite, one observes a plateau for λ as σ varies. It indicates that larger fingers than the ST ones are selected. However, as σ is decreased, λ suddenly falls to 0. A very pronounced crossover occurs between the two regimes. One

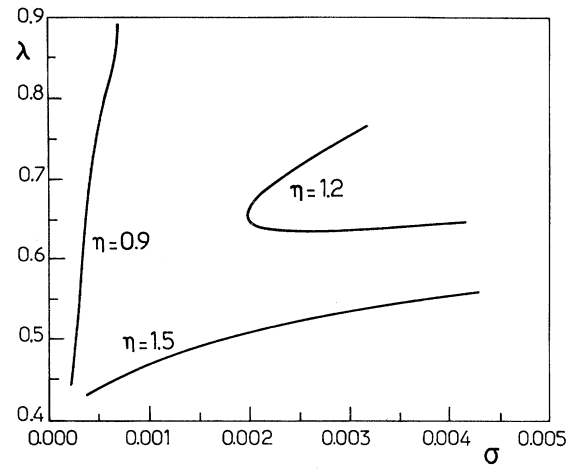


FIG. 2. The angular width λ of the self-similar finger in a sector of 45° . Note the merging of levels for $\eta = 1.2$.

is led to conclude that the vanishing surface tension behavior is completely singular for $\eta = 1$, since the $\lambda = \frac{1}{2}$ limit is only obtained for this value. The radial growth confirms this singular behavior.

When realized at constant flux in a wedge-shaped cell, a self-similar regime in time, in $t^{1/(1+\eta)}$, is found if one neglects σ in a first approximation. Then, it is possible to treat this dynamical growth problem by assuming an adiabatic approximation: the finger has time enough to adjust itself to an effective time-dependent capillary parameter decreasing with time. So as time goes on, the experimental angular finger width describes the λ spectrum. This approximation has been shown to be quantitatively valid as long as λ does not vary too much with σ . Otherwise, it qualitatively gives the main features of the dynamics [10].

In Fig. 2, we show a typical spectrum for a wedge-shaped cell with a sector angle of 45° . This is an intermediate value since we know that the flow becomes more and more unstable with increasing θ_0 . For $\eta = 1.2$, one may observe the usual merging phenomenon of two levels which disappears for $\eta = 0.9$ and $\eta = 1.5$, indicating a stabilizing effect by the selection of a narrow finger: $\lambda \rightarrow 0$. This suggests a competition between the stabilizing $|\eta - 1|$ effect and the destabilization by the divergent flow. Such stabilization never occurs for the ST viscous fingering case since the λ spectrum is characterized by an infinite set of merging phenomena which occur at vanishing surface tension. Of course, for $\eta \neq 1$, this stabilization is related to the small surface tension effect mentioned above for the linear geometry. We arrive at the same conclusion for an anisotropic flow and for a crystal-growth processes [5,10]. So, when $\sigma \rightarrow 0$, the η model behaves like a fourfold anisotropic flow model. This seems rather surprising since the Stefan condition, which acts on the gradient at the interface, is modified while an anisotropy of surface tension modifies the Gibbs-Thomson law that gives the potential on the interface. One can wonder if the formation of needlelike structures at low σ is not the main result of a Laplacian growth process, while the viscous fingering represents an exceptional case where large structures are formed. In the next paragraph, we will try to explain the

vanishing capillary number range in the linear geometry, starting with the second regime after the crossover.

Any attempt to find the zero-surface-tension Laplacian field has been, to our knowledge, unsuccessful. Nevertheless, a first order perturbation analysis can be performed following the conformal mapping techniques; see Bensimon *et al.* [1]. We conformally map the flow domain onto the unit disk $|\omega|=1$ which means that any point in the fluid is described by $z=x+iy=g(\omega,t)$. The image of the interface in the ω plane is the circle and the mapping g is fixed by the modified Stefan condition [Eq. (1)]. In the steady-state approximation, this yields

$$\left[\operatorname{Re} \left(-\omega \frac{dg}{d\omega} \right) \right]^\mu = \operatorname{Re} \left[-\omega \frac{dW}{d\omega} \right] - \omega \frac{dg}{d\omega} \Big|_{\omega=1}^{\mu-1}, \quad (3)$$

with W the complex potential given by $-(V_\infty/\pi)\ln(\omega)$. Equation (3) can be solved perturbatively around the ST field $S(\omega)$ in the limit $\mu \rightarrow 1$. Expanding $g(\omega)$ to first order, $\omega(dg/d\omega) = \omega(dS/d\omega) + (\mu-1)\omega(dh/d\omega)$ in Eq. (3), one easily obtains $\omega(dh/d\omega) = -(\lambda/\pi)\ln[-\pi\omega(dS/d\omega)]$ if $V_\infty = \lambda^\mu$. Of course, to go beyond this approximation is rather difficult, but this expansion suffices and allows us to control the validity of our scaling laws for selection.

We consider the regime of small surface tension σ , where an analytical treatment of the selection process can be performed. We use the technique already employed to describe a variety of physical situations [3,11], which consists of extending the interface equation to the whole fluid phase. The boundary conditions on the interface are then transformed into a differential equation along the finger:

$$\begin{aligned} \sigma \frac{d^2 f}{dz^2} + \frac{1}{2^\mu} f^{(\mu-1)} \left(1 + \frac{1}{f^2} \right)^\mu \\ = \frac{dW}{dz} \approx \lambda^\mu \frac{1+\omega}{1+(2\lambda-1)\omega} \left[1 + (\mu-1) \frac{\lambda(1+\omega)}{1+(2\lambda-1)\omega} \right. \\ \left. \times \ln \left(\frac{1+\omega}{1+(2\lambda-1)\omega} \right) \right], \end{aligned} \quad (4)$$

where $f = e^{i\theta}$, θ being the angle between the normal to the interface and the cell axis and $z = x + iy$ represents any point of the flow. We assume that we can take the zero-surface-tension Laplacian field expanded to first order in $(\mu-1)$ but we retain the differential and local terms on the left-hand side of Eq. (4), which are dominant for the selection process. The numerical results suggest that, after the crossover, a standard spectrum is obtained for small but *finite* σ . So we adapt here the usual treatment and we modify only the scaling laws for the η model.

The curvature term in Eq. (4) acts as a singular perturbation: it becomes important when f becomes singular, when $\lambda^\mu \approx (1/2^\mu) f^{(\mu-1)}$. This happens in the fluid phase, far away from the finger so that ω is small, and the η correction to the ST field is irrelevant. In the neighborhood of this singular point, we introduce rescaled quantities: $\varepsilon = 2^\mu \pi^2 \sigma / 4\mu$, $f = \varepsilon^{-1/(4-\mu)} F$ and, $Y^2 = 2^\mu 2\lambda^\mu (1-\lambda) / \mu \varepsilon^{(3-\mu)/(4-\mu)} \omega$. In reduced variables, Eq. (4) then reads

$$Y \frac{d}{dY} Y \frac{dF}{dY} + F^{\mu-3} = C_\mu + Y^2$$

with

$$C_\mu = \frac{2^\mu \lambda^{\mu-\varepsilon^{(1-\mu)/(4-\mu)}}}{\mu \varepsilon^{(3-\mu)/(4-\mu)}}.$$

C_μ is the usual nonlinear eigenvalue which determines the selection rule between the relative width of the finger λ and the capillary number. In the η model, only a small deviation from the usual ST case can be anticipated if η or μ is close to 1. In this limit, one gets the selection rule:

$$\lambda^\mu \approx \frac{1}{2^\mu} + \frac{\mu}{2^\mu} C_\mu \varepsilon^{(3-\mu)/(4-\mu)} + \frac{1}{2^\mu} \frac{(1-\mu)}{3} \ln(\sigma)$$

when $\sigma \rightarrow 0$.

Of course, this relation assumes that the last term is small so that both σ and $(1-\mu)\ln(\sigma)$ need to be small; so σ cannot be too small. This relation is very similar to the ST selection rule, which is recovered if $\eta = \mu = 1$. It gives also the crossover position which occurs when $(1-\mu)\ln(\sigma)$ is not negligible in comparison to λ , i.e., when $(1-\mu)\ln(\sigma)$ is of order 0.1. The above relation shows that the traditional “ $\lambda \approx \frac{1}{2}$ ” λ value is shifted, and indicates that wider fingers are expected for $\eta < 1$ ($\mu > 1$) and thinner fingers in the opposite situation. If $\eta < 1$, the two corrections to σ act in opposite directions; this effect of compensation explains the plateau observed in Fig. 1. However, in order for this estimate to be valid, σ cannot be too small and cannot reach values of order $10^{-4}, 10^{-3}$ which are common in experiments.

Now, let us try to understand the behavior of λ for very small σ , at fixed η , before the crossover. We assume here that our expansion of the η field remains valid for all values of η . The analysis is different depending on whether η is greater or smaller than 1. For $\eta > 1$ ($\mu < 1$) the leading term on the left-hand side of Eq. (4), when f is singular, is $f^{(\mu-1)}$ which goes to zero. This is consistent with a singular point far away from the finger in the limit $\lambda \rightarrow 0$. The rescaled inner equation we find is not very different from the previous one, if we introduce the rescaled variables: $\varepsilon_1 = \varepsilon\mu$, $f = \varepsilon_1^{-1/(2-\mu)} G$, and $Z^2 = [2^\mu 2\lambda^\mu (1-\lambda) / \varepsilon_1^{(1-\mu)/(2-\mu)}] \omega$,

$$Z \frac{d}{dZ} Z \frac{dG}{dZ} + G^{\mu-1} = D_\mu + Y^2$$

with

$$D_\mu = \frac{2^\mu \lambda^\mu}{\varepsilon_1^{(1-\mu)/(2-\mu)}} \quad \text{so} \quad \lambda \approx \sigma^{(1-\mu)/\mu(2-\mu)}.$$

Like C_μ , D_μ is a nonlinear eigenvalue which can be calculated numerically. It gives the selection rule and the scaling of λ with σ when both σ and $\lambda \rightarrow 0$. Remember that this scaling is valid only for $\eta > 1$ ($\mu < 1$).

The most intriguing situation is the case $\eta < 1$ where an abrupt jump is observed in the λ spectrum, at the crossover in Fig. 1. If λ goes to zero as suggested by the numerical calculations, a boundary layer equation can be obtained only

in the vicinity of the finger tip. However, in this region, probably our zero-surface-tension expansion fails. If we assume it valid, and if W is of order $\lambda^{\mu+1}$, the right-hand side of Eq. (4) is of order 1 so that f remains of order 1. As a consequence z is of order $\lambda^{\mu+1}$ as is W , so that the rescaled equation in the vicinity of the finger tip is

$$E_{\mu} \frac{1}{1+V} \frac{d}{dV} \frac{1}{1+V} \frac{dF}{dV} + \frac{1}{2^{\mu}} F^{(\mu-1)} \left(1 + \frac{1}{F^2} \right)^{\mu} \\ = \frac{1}{1+V} \left(1 + (\mu-1) \frac{1}{1+V} \ln \frac{1}{1+V} \right),$$

with $E_{\mu} = \pi^2/4\lambda^{2(\mu+1)}\sigma$, $F(V) = f(z)$, and $V = \pi/2\lambda^{\mu+1}W$. The scaling law suggested by this equation is

$\lambda \approx \sigma^{1/2(\mu+1)}$ which, unfortunately, is impossible to verify numerically.

To summarize, why $\lambda = \frac{1}{2}$ is never observed for $\eta \neq 1$ appears clearly from the very beginning (Eq. 4). Naively speaking, it is only when $\mu = \eta = 1$ that the constant $\frac{1}{2}$ appears explicitly. No other value is pointed out by Eq. (4). Moreover, the boundary layer necessary to explain the selection mechanism appears only when λ goes to zero.

Here, we have shown that the ideal viscous fingering instability is an exception among all the possible Laplacian growth processes. The most simple nonlinearity one can imagine deeply modifies the physical results. Our numerical results destroy the naive ideas one can have after a decade of extensive studies on an ideal model.

I thank A. Arneodo and D. Bonn for enlightening discussions. Laboratoire de Physique Statistique de l'Ecole Normale Supérieure is associé au CNRS et aux Universités Paris 6 et 7.

-
- [1] P. G. Saffman and G. I. Taylor, Proc. R. Soc. London Ser. A **245**, 312 (1958); P. G. Saffman, J. Fluid Mech. **173**, 73 (1986); G. M. Homsy, Annu. Rev. Fluid Mech. **19**, 271 (1987); D. Bensimon, L. Kadanoff, S. Liang, B. Shraiman, and C. Tang, Rev. Mod. Phys. **58**, 977 (1986); Y. Couder, in *Chaos, Order and Patterns*, edited by R. Artuso, P. Cvitanovic, and G. Casati (Plenum, New York, 1991).
- [2] J. W. Mclean and P. G. Saffman, J. Fluid Mech. **102**, 455 (1981).
- [3] B. I. Shraiman, Phys. Rev. Lett. **56**, 2028 (1986); D. C. Hong and J. S. Langer, *ibid.* **56**, 2032 (1986); R. Combescot, T. Dombre, V. Hakim, Y. Pomeau, and A. Pumir, *ibid.* **56**, 2036 (1986); S. Tanveer, Phys. Fluids **30**, 1589 (1987).
- [4] S. N. Rauseo, P. D. Barnes, and J. V. Maher, Phys. Rev. A **35**, 1245 (1987); H. Thomé, M. Rabaud, V. Hakim, and Y. Couder, Phys. Fluids A **1**, 224 (1989).
- [5] D. Kessler, J. Koplik, and H. Levine, Phys. Rev. A **34**, 4980 (1986); A. T. Dorsey and O. Martin, *ibid.* **35**, 3989 (1987); M. Ben Amar, Europhys. Lett. **16**, 367 (1991).
- [6] J. Nittman, G. Daccord, and H. E. Stanley, Nature (London) **34**, 141 (1985); R. Byron Bird, R. C. Armstrong, and O. Hassager, *Dynamics of Polymer Liquids* (Wiley Interscience, New York, 1987); B. Stuhn, R. Mutter, and T. Albrecht, Europhys. Lett. **18**, 427 (1992).
- [7] L. Niemeyer, L. Pietronero, and H. J. Wiessmann, Phys. Rev. Lett. **52**, 1033 (1984); J. Elezgaray, J. F. Muzy, F. Argoul, and A. Arneodo, *ibid.* **71**, 2425 (1993).
- [8] D. A. Reinelt, Phys. Fluids **30**, 2617 (1987); J. Fluid Mech. **183**, 219 (1987); S. Tanveer, Proc. R. Soc. London Ser. A **428**, 511 (1990).
- [9] M. Ben Amar, Phys. Rev. A **43**, 5702 (1991); **44**, 3673 (1991); Yuhai-Tu, *ibid.* **45**, 1044 (1991).
- [10] R. Almgren, W. S. Dai, and V. Hakim, Phys. Rev. Lett. **71**, 3461 (1993).
- [11] R. Combescot and M. Ben Amar, Phys. Rev. Lett. **67**, 453 (1991); M. Ben Amar, R. Combescot, and Y. Couder, *ibid.* **70**, 3047 (1993).